Accepted Manuscript

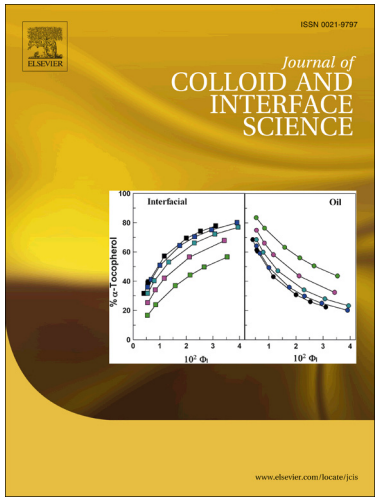

Emulsion-directed liquid/liquid interfacial fabrication of lanthanide ion-doped block copolymer composite thin films

Ming Hong, Yuanyuan Geng, Mei Liu, Yuan Xu, Yong-Ill Lee, Jingcheng Hao, Hong-Guo Liu

PII: S0021-9797(14)00744-9
DOI: http://dx.doi.org/10.1016/j.jcis.2014.09.085
Reference: YJCIS 19893

To appear in: *Journal of Colloid and Interface Science*

Received Date: 30 July 2014
Accepted Date: 28 September 2014

Please cite this article as: M. Hong, Y. Geng, M. Liu, Y. Xu, Y-I. Lee, J. Hao, H-G. Liu, Emulsion-directed liquid/liquid interfacial fabrication of lanthanide ion-doped block copolymer composite thin films, *Journal of Colloid and Interface Science* (2014), doi: http://dx.doi.org/10.1016/j.jcis.2014.09.085

Emulsion-directed liquid/liquid interfacial fabrication of lanthanide ion-doped block copolymer composite thin films

Ming Hong [a], Yuanyuan Geng [a], Mei Liu [a], Yuan Xu [b], Yong-Ill Lee [c], Jingcheng Hao [a], Hong-Guo Liu [a,*]

[a] Key Laboratory for Colloid and Interface Chemistry of Education Ministry, Shandong University, Jinan 250100, P. R. China
[b] School of Chemical Engineering, The University of Queensland, Brisbane, Queensland 4072, Australia
[c] Anastro Laboratory, Department of Chemistry, Changwon National University, Changwon 641-773, Korea

* Corresponding author. Tel: 86-531-88362805; E-mail: hgliu@sdu.edu.cn

ABSTRACT

An emulsion-directed assembly and adsorption approach has been used to fabricate composite films of polystyrene-b-poly(acryl acid)-b-polystyrene (PS-b-PAA-b-PS) and Eu^{3+} and La^{3+} ions at the planar liquid/liquid interface of the polymer DMF/chloroform (1:1, v/v) mixed solution (lower phase) and aqueous solutions of the corresponding salts (upper phase). The lower phase gradually transformed to a water-in-oil (W/O) emulsion via spontaneous emulsification due to the "ouzo effect". Polymer molecules and the metal ions assembled around emulsion droplets that adsorbed at the planar liquid/liquid interface at last, resulting in formation of composite films. The film morphologies and structures depend on Ln^{3+} ions: polymer/Eu^{3+} composite films were foam films composed of microcapsules ranging in size from several hundreds of nanometers to micrometers, while polymer/La^{3+} composite films were composed of hollow spheres several tens of nanometers in size. Fourier transform infrared (FTIR) spectra revealed that the coordination modes of carboxyl groups to Eu^{3+} and La^{3+} were bridging bidentate and ionic, respectively, in the two types of composites. These results indicate that stable microcapsules can be fabricated around droplets for polymer/Eu^{3+} systems, while microcapsules of polymer/La^{3+} are unstable. This leads to different film morphologies and structures. Compositions of these films were characterized using energy-dispersive spectroscopy (EDS) and X-ray photoelectron spectroscopy (XPS). In addition, foam films of polymer/Eu^{3+}/2,2'-bipyridine (bpy) were fabricated using this approach, and their photoluminescence properties were investigated.

Keywords: Liquid/liquid interface; Emulsion; Block copolymer; Adsorption; Composite film; Luminescence

1. Introduction

Composite materials based on polymer matrices have received much attention due to their stability and ease of processing [1]. These composite materials exhibit the intrinsic properties of the components, such as optical and catalytic properties of metal nanoparticles, optical and electronic properties of semiconductor nanoparticles and optical properties of lanthanide complexes. On the other hand, it is possible to emerge new optical, electronic and other properties arising from interactions between polymer and doped components [2]. So it is very important to fabricate polymer-based composite materials. However, homogeneous dispersal of functional species, such as metal ions, metal complexes, small molecules, and inorganic nanoparticles, in polymer matrices remains a great challenge. In order to incorporate these species into polymer matrices, various methods have been proposed and developed [3], such as mixing [4], layer-by-layer assembly [5], electrospinning [6], template-induced polymerization [7], and self-assembly [8].

Recently, adsorption and self-assembly of amphiphilic polymers at the planar liquid/liquid interface have been exploited to fabricate polymer-based composite micro- and nanostructures. Generally, polymer molecules and other species are dissolved in two separate liquid phases. They adsorb and interact with each other at the liquid/liquid interface of these two phases, and further self-assemble into composite micro- and nanostructures. For example, fiber-like nanocomposites composed of CdTe quantum dots and a poly(N-vinylcarbazole) derivative [9], poly(4-vinylpyridine) porous thin films doped with Ag nanoparticles [10], composite nanotubes of a conjugated polymer with Cu^{2+} ions [11], tessellated nanotiles composed of graphene oxide and polystyrene-block-poly(2-vinylpyridine) [12], and polyelectrolyte-surfactant nanocomposite membranes [13] have all been fabricated successfully at liquid/liquid interfaces through adsorption and assembly processes. Though this fabrication method has some limitations, such as requiring polymer to have amphiphilicity, to have functional groups to combine with other components, and to be dissolved into appropriate organic solvents, it has some advantages over other methods mentioned above. For example, this approach enables polymer molecules and other species with different wettability to assemble into composite structures conveniently with various

morphologies under ambient atmosphere, and the combined species disperse homogeneously in the polymer matrices. This method has therefore aroused great research interest.

Besides the progress mentioned above, we have fabricated inorganic species/polymer composites using this approach and obtained various composite structures [14–22]. We dissolved amphiphilic homopolymers or block copolymers in chloroform, and inorganic species, including Ag^+, $AuCl_4^-$, and $PtCl_6^{2-}$ ions, in water. We obtained composite thin films with foam and honeycomb structures, as well as ordered 2D arrays of nanospheres in which noble metal nanoparticles or nanoclusters were homogeneously dispersed after treatment. These composite thin films exhibited high and durable catalytic activity for heterogeneous catalytic reactions due to their unique porous structure and the homogeneous dispersion of metal nanoparticles or nanoclusters.

Polystyrene-block-poly(acrylic acid)-block-polystyrene (PS-b-PAA-b-PS) is a typical amphiphilic block copolymer. It consists of two hydrophobic PS blocks and a hydrophilic PAA block that has carboxyl groups to combine with other species. So it can be applied as a versatile matrix to fabricate various composite materials through the liquid/liquid interfacial adsorption and assembly method. However, the strong polar carboxyl groups make it difficult to dissolve in common organic solvents. To utilize the ability of carboxyl groups to coordinate with metal ions to fabricate composite structures at the interface, PS-b-PAA-b-PS was dissolved in DMF/chloroform mixed solvents. Very recently, we found that W/O emulsions formed in the organic phase after formation of planar interfaces of a DMF/chloroform (1:1) solution of polymer and aqueous solutions of lead acetate or cadmium acetate, due to the "ouzo effect" arising from the solubility of DMF in water. Polymer molecules and metal cations (Cd^{2+} and Pb^{2+}) assembled around the emulsion droplets, and thin composite foam films were generated at the planar liquid/liquid interfaces as a result of adsorption of the polymer molecule-surrounded droplets. CdS and PbS nanoclusters were generated after treatment [23]. In addition, thermo-sensitive and catalytically active PS-b-PAA-b-PS/Ag composite thin films were fabricated successfully using the same approach [24]. This represents an extended liquid/liquid interfacial adsorption and assembly approach involving emulsion droplet-directed assembly and adsorption processes. To examine the universality of this method, and to fabricate more foam-like functional composite microstructures, we

fabricated composite films of PS-b-PAA-b-PS with lanthanide ions (La^{3+} and Eu^{3+}) in this paper. Lanthanide elements have excellent optical and other properties, and lanthanide ion- and complex-doped polymer composites have been intensively researched over the past several decades. Various composites have been prepared and their properties, especially luminescent properties, have been investigated [25–33]. New methods to fabricate polymer-based composites in which lanthanide ions or complexes are homogeneously dispersed are therefore in great demand.

We found that lanthanide ions have a large effect on the microstructure of the formed composite films: PS-b-PAA-b-PS/Eu^{3+} foam films were composed of microcapsules that formed around emulsion droplets, while films containing La^{3+} were composed of smaller hollow spheres contributed by micelles and vesicles. We attributed these distinct assembly behaviors to the different coordination abilities of La^{3+} ions and Eu^{3+} ions with carboxyl groups. In addition to the Ln^{3+} ion-doped composites, we fabricated europium complex-doped polymer foam films using this method by simply adding the ligand, 2,2'-bipyridine (bpy) to the organic phase. The photoluminescent intensity of the complex-doped thin film was significantly higher than that of the Eu^{3+}-doped thin film. In comparison with other methods, such as mixing one, this method can fabricate metal ions and ligands directly during the assembly process, reflecting convenience and feasibility of this method. We also anticipate that more and more functional composite films composed of various amphiphilic polymers and other species can be fabricated through this emulsion-directed adsorption and assembly approach.

2. Experimental section

2.1. Chemicals

PS-b-PAA-b-PS with M_n values for the three blocks of 3000, 8000, and 3000 g mol^{-1} (M_w/M_n = 1.35) was purchased from Polymer Source (Canada) and used as received. Europium oxide (Eu_2O_3, 99.99%, Shanghai Yuelong Chemical Plant), europium nitrate hexahydrate ($Eu(NO_3)_3 6H_2O$, 99.99%, Sun Chem. Tech. (Shanghai) Co., Ltd.), lanthanum

nitrate hexahydrate ($La(NO_3)_3 6H_2O$, 98%, Beijing Xuanwu Chemical Plant), and lanthanum perchlorate hexahydrate ($La(ClO_4)_3 6H_2O$, Alfa Aesar) were used as received. 2,2'-bipyridine (bpy) was obtained from Shanghai Chemical Plant. Chloroform (analytical reagent) containing 0.3-1.0% ethanol as a stabilizer was obtained from Tianjin Guangcheng Chemical Company. The water used was highly purified using an ultra-pure water purification system (UPHW-IV-90T, Chengdu China) with a resistivity ≥18.0 MΩ cm.

2.2. Formation of composite films at liquid/liquid interfaces

A certain amount of PS-b-PAA-b-PS was dissolved in DMF first under ultrasonication, and then a certain amount of chloroform was added to form a mixed solution. Unless otherwise specified, the volume ratio of DMF to chloroform in the mixed solution was 1:1, and the concentration of the polymer was 0.20 mg mL^{-1}. Mixed organic solution of PS-b-PAA-b-PS/bpy was prepared by adding a certain amount of bpy to the 1:1 solution. The concentration of bpy was 0.10 mg mL^{-1}.

Aqueous solutions of lanthanum nitrate, lanthanum perchlorate, and europium nitrate of 1×10^{-2} mol L^{-1} and mixed aqueous solutions of $La(NO_3)_3/Eu(NO_3)_3$ with different molar ratios of La/Eu were prepared by directly dissolving the corresponding salts in pure water. Aqueous solution of europium perchlorate of 1×10^{-2} mol L^{-1} was first prepared by completely dissolving europium oxide in perchloric acid, evaporating redundant perchloric acid, and then adding a certain amount of water.

Approximately 5 mL of the polymer solution was poured into a clean and dry bottle. Then, an equal volume of the aqueous solution was added slowly along the bottom wall by using a pipette to cover the organic solution. A clear planar liquid/liquid interface formed. The organic and the aqueous phases were called the lower and upper phases, respectively. Mass transfer across the interface took place immediately when the interface formed. Gradually, the interface became unclear and the lower phase became milky. A thin film appeared at the interface when the lower phase became clear again. The thin film was deposited onto solid substrates, such as carbon-coated copper grids and quartz slides, after the upper phase was removed with a dropper.

2.3. Characterization of composite films

Deposited films from the liquid/liquid interfaces were characterized using various techniques. Morphology and structure of the thin films deposited on copper grids were investigated using a high-resolution transmission electron microscope (HRTEM, JEOL-2010) with an accelerating voltage of 200 kV. Element analysis was carried out using an energy-dispersive spectroscope (EDS; Oxford INCAx-sight) attached to the HRTEM. Compositions of the samples were probed by X-ray photoelectron spectroscopy (XPS, ESCALAB MKII) with an Mg Kα excitation source at a pressure of 1.0×10^{-6} Pa and resolution of 1.00 eV. In order to clarify the interaction between polymer molecules and metal ions, the thin films that formed at the liquid/liquid interfaces were investigated by FTIR spectroscopy (VERTEX-70). Thin films were deposited on glass slides first, and then scraped from the slides after drying. Films pieces were collected and FTIR spectra were obtained with KBr pellet pressing. Photoluminescence (PL) spectra of the thin films containing europium were obtained using a PL spectroscope (F-7000, Hitachi) at an excitation wavelength of 260 nm at room temperature.

2.4. Dynamic light scattering (DLS) measurements

The lower phase changed from a clear organic solution to a cloudy dispersion and then to a clear solution again during the assembly process. To study this change, the lower phase was monitored using a DLS technique with a BI-200SM research goniometer and laser light scattering system (Brookhaven Instruments Corporation, USA). An argon laser (λ= 532 nm) with variable intensity was used to cover the size range involved. Measurements were carried out at a scattering angle of 90° at room temperature.

2.5. Freeze fracture TEM (FF-TEM) observations

A small amount of emulsion in the lower phase was placed on a 0.1-mm-thick copper disk

and then covered with a second copper disk. The copper sandwich with the sample was then plunged into liquid nitrogen. Fracturing and replication were carried out on Balzers BAF-400D equipment at -150℃. Pt/C was deposited at an angle of 45°. Replicas were examined on a JEOL-2010 HRTEM with an accelerating voltage of 200 kV.

3. Results and discussion

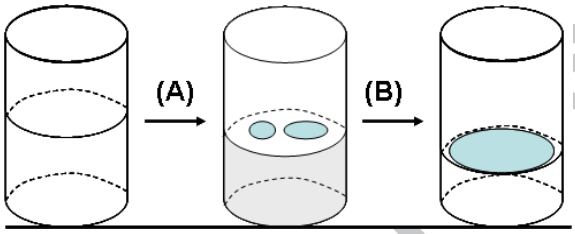

Scheme 1. Schematic representation of composite thin film formation at the planar liquid/liquid interface through emulsion-directed assembly and adsorption processes. (A) Emulsification of the lower phase and self-assembly templated by the droplets; (B) adsorption at the liquid/liquid interface and formation of a thin film.

In our previous report [23], we found that W/O emulsion formed gradually in the organic phase after formation of the planar liquid/liquid interface of a DMF/chloroform solution of PS-b-PAA-b-PS and an aqueous solution of Cd^{2+} or Pb^{2+}. The emulsion droplets acted as templates to assemble the polymer molecules, polymer micelles, and metal ions aided by coordination interactions between carboxyl groups and cations. Composite droplets finally adsorbed at the planar liquid/liquid interface, resulting in the formation of a composite foam film, as illustrated in Scheme 1.

Because various interactions between carboxyl groups and metal ions are possible, various composite foam films can be fabricated using the emulsion-directed assembly and adsorption approach. We fabricated PS-b-PAA-b-PS/Ln^{3+} composite films by replacing aqueous solutions of Cd^{2+} and Pb^{2+} with Ln^{3+}. As expected, an emulsion formed gradually after formation of the planar liquid/liquid interface. The milky lower phase became clear and a thin

film appeared at the interface after a certain time. Formation and evolution of the lower phase emulsion were monitored using DLS, as shown in Fig. 1. A distribution peak with a mean hydrodynamic diameter of 29 nm appeared in the DLS spectrum of the DMF/chloroform solution, indicating micelle formation. In addition, a shoulder appeared at 69 nm, suggesting the presence of larger micelles or vesicles. Multimodal distribution peaks with mean hydrodynamic diameters of 38, 340, and 1100 nm appeared in the DLS spectra of the milky lower phase, corresponding to the sizes of micelles and emulsion droplets, respectively, and indicating the preservation of micelles and formation of emulsions. Please note that the band centered at 38 nm is broad, ranging from 20 to 110 nm, indicating the existence of larger aggregates, such as vesicles. After the lower phase became clear, the peak corresponding to the emulsion droplets became very weak, indicating that most of the droplets adsorbed at the planar interface to form the thin composite film. An FF-TEM image of the lower phase emulsion is provided in Fig. 2. Numerous hollow spheres with diameters of ~26 nm and some larger hollow spheres with diameters ranging from several hundred nanometers to micrometers appeared which correspond to micelles and emulsion droplets, respectively. Some smaller hollow spheres with the size ranging from 50 to 80 nm can be observed from Fig. 2b, indicating the existence of vesicles. DLS and FF-TEM results were consistent with each other, confirming the coexistence of micelles, vesicles and droplets in the lower phase emulsion.

The formation of the emulsion in the lower phase was attributed to a spontaneous emulsification process related to the “ouzo effect” [34-37]. DMF migrates to the aqueous phase and the aqueous solution simultaneously migrates to the organic phase after formation of the liquid/liquid interface. At the early stage of migration, the lower phase keeps clear due to the miscibility of DMF with water and chloroform. Water droplets nucleate in the lower phase gradually as the amount of water increases and the amount of DMF decreases with time, and grow through an Ostwald ripening process [35], leading to formation of a W/O emulsion. The dispersion and continuous phases in the emulsion are aqueous solution droplets and polymer organic solution, respectively. The micelles, vesicles, together with the free polymer molecules in the continuous phase, adsorbed around the droplets, and combined with the Ln^{3+} ions in the droplets to form microcapsules. The microcapsules can be regarded as solid shells

around the droplets, which adsorbed at the planar liquid/liquid interface due to their different wettability to aqueous and oil phases, resulting in the formation of a composite thin layer.

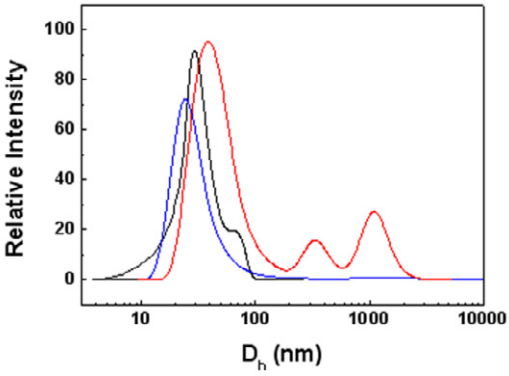

Fig. 1. DLS spectra of the polymer DMF/chloroform solution (black), the milky lower phase (red), and the clear lower phase after fabrication (blue) of the polymer/La^{3+} system.

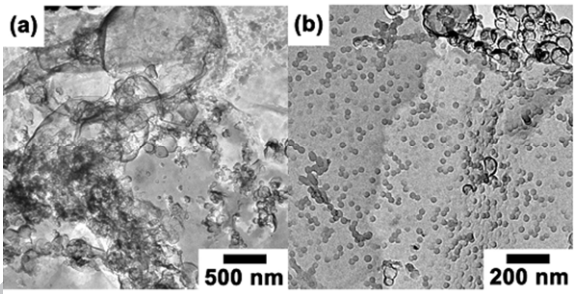

Fig. 2. FF-TEM micrographs of the milky lower phase in the polymer/La^{3+} system.

Fig. 3 shows TEM images of the composite films of PS-b-PAA-b-PS/Eu^{3+} and PS-b-PAA-b-PS/La^{3+}. EDS spectra of these composite films (Fig. S1 in the supporting information) show clear Eu and La signals, indicating that lanthanide ions were successfully incorporated into the composite films. As shown in Fig. 3a,b, composite films containing Eu^{3+} had a foam-like structure, consisting of small, hollow spheres with diameters ranging from 20 to 50 nm that decorated the walls. This structure is similar to those of composite films containing Cd^{2+} and Pb^{2+}. Numerous inorganic nanoclusters ranging between 1 −2 nm were visible in the walls. However, to our surprise, aggregates of spheres several hundreds of nanometers to micrometers in size appeared at the interface for the polymer/La^{3+} system

rather than a foam structure, as shown in Fig. 3c. A high-magnification image (Fig. 3d) indicated that the spheres were composed of numerous superimposing smaller hollow spheres with a size between 20 and 30 nm. These two distinct structures reflect different formation mechanisms. The polymer/Eu^{3+} system provided results that were expected for the emulsion droplet-directing assembly and adsorption approach, while the polymer/La^{3+} system did not produce the expected outcome. This indicates that metal ions have a large impact on the assembly behavior and final structure of thin films obtained using this approach.

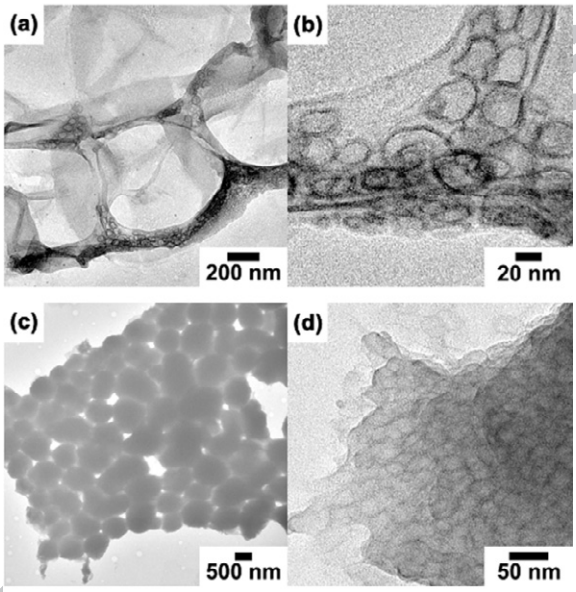

Fig. 3. TEM micrographs of composite polymer/Eu^{3+} (a, b) and polymer/La^{3+} (c, d) films.

To confirm this effect further, composite films containing Eu^{3+} and La^{3+} ions were fabricated by replacing nitrates with perchlorates. TEM images of these composite films are shown in Fig. S2. The composite structure containing Eu^{3+} comprised foam decorated with smaller hollow spheres, while the composite structure containing La^{3+} was composed of smaller hollow spheres. These microstructures resembled those obtained when using nitrates. This demonstrates that lanthanide cations strongly influence the assembly behaviors of polymer molecules and their final structures.

Fig. S3 shows TEM micrographs and EDS spectra of composite films formed at the liquid/liquid interfaces between DMF/$CHCl_3$ polymer solution and mixed aqueous solutions

of $Eu(NO_3)_3$ and $La(NO_3)_3$ with Eu/La molar ratios of 80:20, 50:50, and 20:80. Foam structures formed for all of these systems. Actual molar ratios of Eu/La in the composite films were measured using EDS and found to be 87:13, 66:34, and 42:58, respectively, which are higher than those in aqueous solutions, implying that Eu^{3+} is more inclined to interact with carboxyl groups than La^{3+}. In other words, Eu^{3+} ions dominate the assembly process for these mixed systems, leading to the formation of foam films.

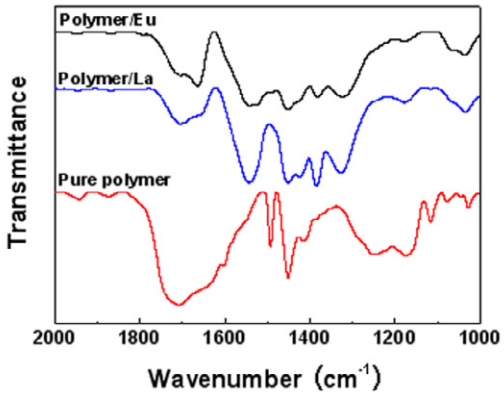

Fig. 4. FTIR spectra of pure polymer and polymer composites.

The different assembly behaviors of PS-b-PAA-b-PS with La^{3+} and Eu^{3+} are likely related to different interactions between the polymer molecules and lanthanide ions. We evaluated this hypothesis using FT-IR spectroscopy. FT-IR spectra of the composites and pure polymer are shown in Fig. 4. We assigned the broad band at 1707 cm^{-1} and the weak band at 1943 cm^{-1} to C=O stretching vibrations and the satellite band of the stretching vibrations of hydrogen-bonded hydroxyl groups, respectively; these peaks indicate that the polymer was in an associated state through hydrogen bonding [38,39]. We attributed the strong shoulder around 1650 cm^{-1} to the H-O-H deformation mode of physically adsorbed water [40,41], and the broad band at 1255 cm^{-1} to C-O stretching coupled with O-H in-plane bending [42]. Other vibration bands at 1452, 1493, and 1600 cm^{-1} in the spectra of the composites are characteristic of PS block vibrations [43-45]. However, peaks related to PAA blocks differed between the composites and the pure polymer. Although bands corresponding to C=O stretching vibrations of the COOH groups still appeared at 1705 cm^{-1} in the spectra of the

composites, their intensity decreased, and the broad band at 1255 cm^{-1} almost disappeared. Simultaneously, two new bands appeared at 1544 and 1384 cm^{-1} in the spectrum of the polymer/La^{3+} composite, and at 1545-1520 and 1382 cm^{-1} in the spectrum of the polymer/Eu^{3+} composite; we assigned these to asymmetric and symmetric stretching vibrations of COO^-, respectively [46,47]. These results indicate that two kinds of carboxyl groups, undissociated COOH groups and dissociated COO^- groups that coordinated with Ln^{3+} ions were present in the two types of composites.

We identified differences in the asymmetric stretching vibrations of COO^- groups in the two kinds of composites. For the composite containing La^{3+}, this band was centered at 1544 cm^{-1}, while for the composite containing Eu^{3+}, this band was broader with a shoulder at 1520 cm^{-1}. The frequency difference, $\Delta\nu = \nu_{as}(COO^-) - \nu_s(COO^-)$, has been used as an empirical criterion to deduce the coordination mode between COO^- groups and metal ions [48,49]. The $\Delta\nu$ value for the polymer/La^{3+} composite was 160 cm^{-1}, while that for the polymer/Eu^{3+} composite was 138 –163 cm^{-1}. This indicates that the coordination type between COO^- and La^{3+} is ionic. Although ionic coordination cannot be excluded for the COO^- to Eu^{3+} interaction, the coordination type for this polymer is more likely to be bridging bidentate. Because ionic bonds can be broken easily, adsorbed layers around the emulsion droplets are not very stable. It is therefore difficult to obtain a foam structure at the planar liquid/liquid interface for PS-b-PAA-b-PS/La^{3+}. In contrast, more stable layers can form around emulsion droplets through bridging bidentate coordination between carboxyl groups and Eu^{3+} ions, resulting in the formation of foam films. It is not clear why La^{3+} and Eu^{3+} adopted different coordination modes with carboxyl groups. This may be related to the lanthanide contraction effect. It should be mentioned that different coordination modes between lanthanide ions and carboxyl groups have been reported in different systems, likely due to different carboxyl types and microenviroenments [50-52].

It is well known that some ligands, such as 2,2'-bipyridine, 1,10-phenanthroline, and βdiketone form complexes with lanthanide ions. They can transfer absorbed energy to central lanthanide ions, such as Sm^{3+}, Eu^{3+}, and Tb^{3+}, to enhance the luminescence of these ions. This is the so-called "antenna effect". We added bpy to the polymer DMF/chloroform solution and fabricated composite films of polymer/Eu^{3+}/bpy. We expected that bpy would coordinate with

Eu^{3+} during the assembly process.

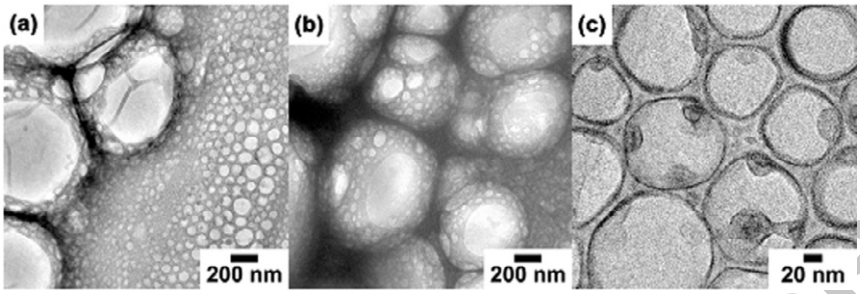

Fig. 5. TEM micrographs of the polymer/Eu^{3+}/bpy composite film formed at the liquid/liquid interface of the polymer/bpy mixed DMF/chloroform solution and $Eu(NO_3)_3$ aqueous solution.

The morphology of the composite films formed at the planar liquid/liquid interface is shown in Fig. 5. Compared with the foam structures without bpy shown in Fig. 1 and Fig. S3, the composite films of polymer/Eu(III)/bpy had some new structural features. Two types of microstructures were visible in the TEM images. One was homogeneous film composed of hollow spheres with diameters ranging from several tens of nanometers to one hundred nanometers. The other was microcapsules several hundreds of nanometers in size. Walls of the microcapsules were composed of hollow spheres. Wall thickness of the hollow spheres was approximately 9 nm based on the high magnification image (Fig. 5c), which is much thinner than the thickness of the microcapsules. We reasoned that these hollow spheres were vesicles that preformed in the organic phase. In addition, micellar structures with the size of about 30 nm that attached on the vesicles can be observed in Fig. 5c.

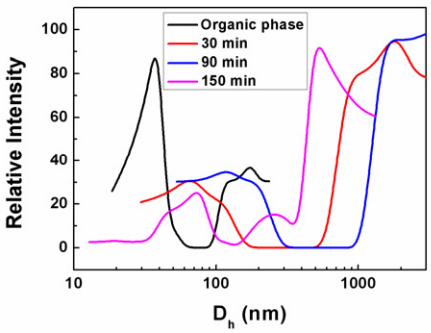

Fig. 6. DLS spectra of the polymer/bpy DMF/chloroform mixed solution, the lower phase after the formation of the liquid/liquid interface for 30, 90 and 150 min.

Fig. 6 shows the DLS spectra of the polymer/bpy mixed solution and the lower phase after the formation of the liquid/liquid interface at different time. Two distribution bands with mean hydrodynamic diameters of 37 and 172 nm appeared in the spectrum of the mixed organic solution, indicating two kinds of aggregates, i.e. micelle and vesicle existed in the solution. Compared with the spectrum of the organic solution without bpy, the proportion of vesicle increased, indicating more vesicles formed in the mixed solution. It can be seen from the DLS spectra that multimodal distribution bands with the mean hydrodynamic diameters of several tens of nanometers, one hundred to two hundreds of nanometers and from 500 to 1700 nm appeared during the emulsification process, suggesting the generation of emulsion droplets and the existence of micelles and vesicles. These micelles and vesicles adsorbed on the droplets and at the planar liquid/liquid interface at last, resulting in the formation of a foam film composed of microcapsules whose walls were composed of hollow spheres, and the formation of a homogeneous film composed of smaller hollow spheres and round aggregates, as shown in Fig. 5.

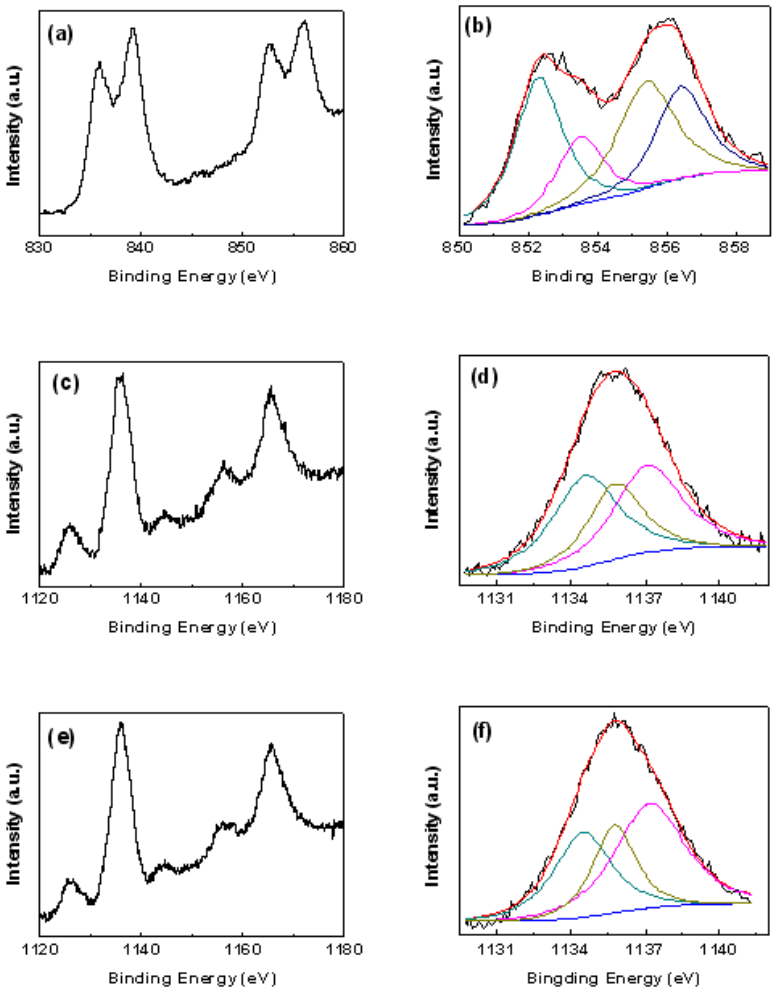

Fig. 7. XPS spectra of composites containing La(III) (a, b), Eu(III) (c, d), and Eu(III)/bpy (e, f).

Film compositions were analyzed based on XPS spectra (Fig. 7). The spectrum of the polymer/La^{3+} composite exhibited characteristic bands of $La3d_{5/2}$ at 836.1 eV and $La3d_{3/2}$ at 852.5 eV, together with their satellite bands at 839.0 and 856.0 eV, respectively. The $La3d_{3/2}$ band and its satellite band were decomposed into two peaks, respectively, as shown in Fig. 7b, indicating the presence of at least two kinds of species, namely hydrolyzed and coordinate species.

Fig. 7c and Fig. 7e show the characteristic doublet of Eu(III) 3d levels. $Eu3d_{5/2}$ bands were found at 1135.7 eV with a satellite at 1125.8 eV for the polymer/Eu^{3+} composite without bpy, and 1135.7 eV with a satellite at 1126.0 eV for the polymer/Eu^{3+}/bpy composite. $Eu3d_{3/2}$

bands and their satellites also appeared in these spectra. These bands were asymmetric. $Eu3d_{5/2}$ bands for these two composites were decomposed into three peaks at 1134.7, 1135.8, and 1137.2 eV, and at 1134.5, 1135.8, and 1137.2 eV, respectively. This suggests that three kinds of species, corresponding to hydrolyzed Eu_2O_3, $Eu(OH)_3$, and coordinated Eu(III), respectively, exist in these composites [53-56]. The hydrolyzed species formed nanoclusters, as can be seen in the high-magnification TEM images.

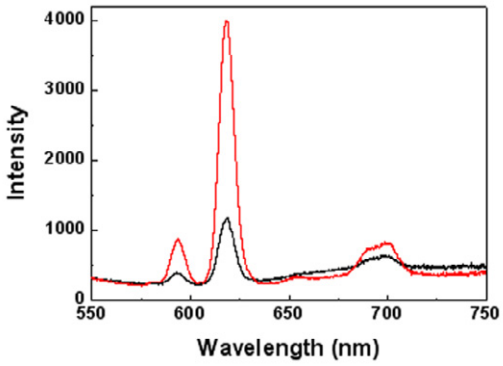

Fig. 8. Photoluminescence spectra of polymer/Eu(III) (black) and polymer/Eu(III)/bpy (red) composite thin films at an excitation wavelength of 260 nm.

Composite films produced characteristic fluorescent peaks of Eu(III) under UV-light excitation, as shown in Fig. 8. Three bands centered at 593, 618, and 700 nm appeared in the curve of the polymer/Eu^{3+} composite, which we ascribed to $^5D_0 \rightarrow {}^7F_1$, $^5D_0 \rightarrow {}^7F_2$, and $^5D_0 \rightarrow {}^7F_4$ transitions, respectively. Besides the bands corresponding to these transitions, two weak bands were present at 581 and 653 nm in the curve of the polymer/Eu^{3+}/bpy composite, corresponding to $^5D_0 \rightarrow {}^7F_0$ and $^5D_0 \rightarrow {}^7F_3$ transitions, respectively. The two composite films were prepared under the same conditions, and they were of similar thicknesses. The intensity of the $^5D_0 \rightarrow {}^7F_2$ hypersensitive transition band of Eu(III) in the polymer/Eu^{3+}/bpy composite was much stronger than that in the composite without bpy, indicating that ligand molecules were assembled into the composite successfully during the fabrication process.

The luminescence properties of Eu(III) in complexes with PAA [57-59] and composite structures formed by PAA, such as hydrogels [60] have been investigated. It was reported that the luminescence of the PAA/Eu composite hydrogel was stronger than that of aqueous

solution of europium nitrate due to the expulsion of water molecules from the salvation shell of Eu^{3+} ions. The ratio of $I(^5D_0 \rightarrow {}^7F_2)/I(^5D_0 \rightarrow {}^7F_1)$ increased from 0.41–0.63 of the aqueous solutions to 3.3–3.5 of the composite hydrogels, indicating that Eu^{3+} was located in an asymmetric central in the hydrogel [60]. The stoichiometric complex of PAA/Eu also exhibited stronger luminescence with a $I(^5D_0 \rightarrow {}^7F_2)/I(^5D_0 \rightarrow {}^7F_1)$ ratio of 2.52, which was ascribed to the coordination of the carboxylate to Eu^{3+} in a bidentate form and the energy transfer from the polymer matrix to Eu^{3+} ions [57]. It was demonstrated that the coordination types have great influences on luminescent properties of Eu^{3+}: bidentate coordination mode promotes the lanthanide ion luminescence intensification [59].

The luminescence intensity of the PS-b-PAA-b-PS/Eu composite film obtained at the liquid/liquid interface is similar to that of the stoichiometric complex of PAA/Eu [57], while the $I(^5D_0 \rightarrow {}^7F_2)/I(^5D_0 \rightarrow {}^7F_1)$ ratio was found to be 5.52, obviously larger than 2.52, that of the PAA/Eu complex, indicating that Eu^{3+} ion was in a more asymmetric central in the film. It can be also seen that this ratio is larger than that of Eu^{3+} in the composite hydrogel [60]. The FTIR spectral analysis indicated that the carboxylate coordinated to Eu^{3+} in the composite film in a bidentate form, which would enhance the luminescence of the central ions [59]. In addition, the second ligand, bpy enhanced the luminescence of the PS-b-PAA-b-PS/Eu/bpy composite film further. Furthermore, the emulsion-directed assembly and adsorption process ensured the homogeneously dispersion of Eu^{3+} ions in the composite films, preventing the concentration quenching of the luminescence effectively. Therefore, this method is a convenient and useful one to construct composite structures containing Eu^{3+} and Eu(III) complexes with good luminescence performance.

We also examined the effects of fabrication conditions on the microstructures that formed in the films. For example, two-dimensional ordered arrays were obtained by changing the DMF/chloroform volume ratios of polymer solution from 1:1 to 1:3, as shown in Fig. 9. Round nanoplates with a mean diameter of about 100 nm formed at the liquid/liquid interface. These nanoplates were composed of round nanodots about 10 nm in size that formed a two-dimensional array in each nanoplate. These nanodots likely correspond to reverse micelles formed by polymer molecules in DMF/chloroform (1:3) solution due to the increase in chloroform, which is a poor solvent for PAA blocks. These reverse micelles adsorbed at the

planar liquid/liquid interface, and Eu^{3+} ions were incorporated into the center of these reverse micelles during this process. This indicates that various microstructures can be fabricated using the approach described in this paper by altering fabrication conditions.

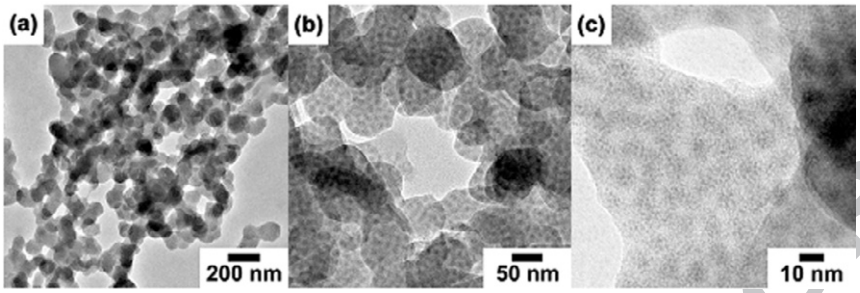

Fig. 9. TEM micrographs of polymer/Eu^{3+} composites formed at the interface of the polymer DMF/chloroform (1:3) solution and $Eu(NO_3)_3$ aqueous solution.

4. Conclusion

We successfully fabricated PS-b-PAA-b-PS/Eu^{3+} and PS-b-PAA-b-PS/Eu^{3+}/bpy composite foam films at planar liquid/liquid interfaces through emulsion-directed assembly and adsorption processes. These thin films exhibited characteristic photoluminescence properties of Eu(III). However, PS-b-PAA-b-PS/La^{3+} composite films composed of small, hollow spheres instead of a foam structure formed using the same approach. This reflects different fabrication mechanisms for these composites and highlights the significant effects of metal ions on the fabrication processes and the final structures. We attributed these differences to different coordination modes of carboxyl groups to Eu^{3+} and La^{3+} ions. Interactions between polymer molecules and inorganic species should be carefully considered when using an emulsion-directed assembly and adsorption method for composite fabrication.

Acknowledgment

This work was supported by grants from the National Natural Science Foundation of China (No. 21273133 and 21033005).

References

[1] H. Zhang, J. Han, B. Yang, Adv. Funct. Mater. 20 (2010) 1533–1550.

[2] B. K. Kuila, A. Garai, A. K. Nandi, Chem. Mater. 19 (2007) 5443−5452.

[3] J. Wang, W. Li, J. Zhu, Polymer 55 (2014) 1079–1096.

[4] S. G. Jang, E. J. Kramer, C. J. Hawker, J. Am. Chem. Soc. 133 (2011) 16986–16996.

[5] B. Lee, Y. Kim, S. Lee, Y. S. Kim, D. Wang, J. Cho, Angew. Chem. Int. Ed. 49 (2010) 359–363.

[6] S. Kundu, R. S. Gill, R. F. Saraf, J. Phys. Chem. C 115 (2011) 15845–15852.

[7] G. Zotti, B. Vercelli, A. Berlin, P. T. K. Chin, U. Giovanella, Chem. Mater. 21 (2009) 2258–2271.

[8] H. Zhang, Y. Liu, D. Yao, B. Yang, Chem. Soc. Rev. 41 (2012) 6066–6088.

[9] S. Yang, C.-F; Wang, S. Chen, J. Am. Chem. Soc. 133 (2011) 8412–8415.

[10] Z. B. Ren, J. Liu, Y. P. Chen, M. Chen, D. J. Qian, Chin. Chem. Lett. 22 (2011) 867–870.

[11] C. Zhou, N; Chen, J. Yang, H; Liu, Y. Li, Macromol. Rapid Commun. 33 (2012) 688–692.

[12] Z. Sun, T. Feng, T. P. Russell, Langmuir 29 (2013) 13407–13413.

[13] D. B. Carew, K. J. Channon, I. Manners, D. N. Woolfson, Soft Matter 7 (2011) 3475–3481.

[14] L.-J. Chen, H. Ma, K. Chen, H.-R. Cha, Y.-I. Lee, D.-J. Qian, J. Hao, H.-G. Liu, J. Colloid Interface Sci. 362 (2011) 81–88.

[15] L.-J. Chen, H. Ma, K.-C. Chen, W. Fan, H.-R. Cha, Y.-I. Lee, D.-J. Qian, J. Hao, H.-G. Liu, Colloids Surf., A 386 (2011) 141–150.

[16] L. Lin, K. Shang, X. Xu, C. Chu, H. Ma, Y.-I. Lee, J. Hao, H.-G. Liu, J. Phys. Chem. B 115 (2011) 11113–11118.

[17] C. Chu, D. Yang, D. Wang, H. Ma, H.-G. Liu, Mater. Chem. Phys. 132 (2012) 916–922.

[18] H. Ma, Y. Geng, Y.-I; Lee, J. Hao, H.-G. Liu, J. Colloid Interface Sci. 394 (2013) 223–230.

[19] H. Ma, Y. Geng, Y.-I. Lee, J. Hao, H.-G. Liu, Colloids Surf., A 419 (2013) 201–208.

[20] D. Wang, H. Ma, C. Chu, J. Hao, H.-G. Liu, J. Colloid Interface Sci. 402 (2013) 75–85.

[21] Y. Liu, L. Chen, Y. Geng, Y.-I. Lee, Y. Li, J. Hao, H.-G. Liu, J. Colloid Interface Sci. 407 (2013) 225–235.

[22] C. Chu, D. Wang, H. Ma, M. Yu, J. Hao, H.-G. Liu, Mater. Chem. Phys. 142 (2013) 259–267.

[23] Y. Geng, M. Liu, K. Tong, J. Xu, Y.-I. Lee, J. Hao, H.-G. Liu, Langmuir 20 (2014) 2178–2187.

[24] M. Liu, Q. Wang, Y. Geng, C. Wang, Y.-I. Lee, J. Hao, H.-G. Liu, Langmuir 30 (2014) 10503–10512.

[25] K. Binnemans, Chem. Rev. 109 (2009) 4283-4374.

[26] K. S. V. K. Rao, H.-G. Liu, Y.-I. Lee, Appl. Spectroscopy Rev. 45 (2010) 409-446.

[27] Q. Lai, H. Lu, D. Wang, H. Wang, S. Feng, J. Zhang, Macromol. Chem. Phys. 212 (2011) 1435–1442.

[28] K. Lunstroot, K; Driesen, P. Nockemann, L. Viau, P. H. Mutin, A. Vioux, K. Binnemans, Phys. Chem. Chem. Phys. 12 (2010) 1879–1885.

[29] M. Tsvirko, E. Mandowska, M. Biernacka, S. Tkaczyk, A. Mandowski, J. Lumin. 143 (2013) 128–131.

[30] K. Buczko, M. Karbowiak, J. Lumin. 143 (2013) 241–253.

[31] H. Liang, F. Xie, J. Lumin. 144 (2013) 230–233.

[32] J. Xu, Y; Ma, L; Jia, X; Huang, Z. Deng, H. Wang, W. Liu, Y. Tang, Mater. Chem. Phys. 133 (2012) 78–86.

[33] X. Wang, S. Zhou, L. Wu, Mater. Chem. Phys. 137 (2012) 644-651.

[34] D. J. McClements, Soft Matter 7 (2011) 2297–2316.

[35] S. A. Vitale, J. L. Katz, Langmuir 19 (2003) 4105–4110.

[36] N. L. Sitnikova, R. Sprik, G. Wegdam, E. Eiser, Langmuir 21 (2005) 7083–7089.

[37] M. Kowacz, J. M. S. S. Esperança, L. P. N. Rebelo, Soft Matter 10 (2014) 3798–3805.

[38] E. Hao, T. Lian, Chem. Mater. 12 (2000) 3392–3396.

[39] Y. Chen, Y. Pang, J. Wu, Y. Su, J. Liu, R. Wang, B. Zhu, Y. Yao, D. Yan, X. Zhu, Q. Chen, Langmuir 26 (2010) 9011-9016.

[40] F. Barroso-Bujans, R. Serna, E. Sow, J. L. G. Fierro, M. Veith, Langmuir 25 (2009) 9094–9100.

[41] H. A. Al-Abadleh, V. H. Grassian, Langmuir 19 (2003) 341–347.

[42] J. S. Shaikha, R. C. Pawara, A. V. Moholkarb, J. H. Kimb, P. S. Patil, Appl. Surf. Sci.

257 (2011) 4389-4397.

[43] S. G. Boyes, B. Akgun, W. J. Brittain, M. D. Foster, Macromolecules 36 (2003) 9539-9548.

[44] B. Su, Z. Ma, S. Min, S; She, Z. Wang, Mater. Sci. Eng. A 458 (2007) 44-47.

[45] C.-C. Tseng, C.-P. Chang, Y. Sung, J.-L. Ou, M.-D. Ger, Colloids Surf. A 333 (2009) 138–144.

[46] Y. El Khoury, P. Dorlet, P. Faller, P. Hellwig, J. Phys. Chem. B 115 (2011) 14812–14821.

[47] R. Dong, M; Lindau, C. K. Ober, Langmuir 25 (2009) 4774-4779.

[48] J. Simon-Kutscher, A. Gericke, H. Huhnerfuss, Langmuir 12 (1996) 1027–1034.

[49] C. Ohe, H. Ando, N. Sato, Y. Urai, M. Yamamoto, K. Itoh, J. Phys. Chem. B 103 (1999) 435-444.

[50] T. Hemraj-Benny, S. Banerjee, S. S. Wong, Chem. Mater. 16 (2004) 1855–1863.

[51] C. Wan, M. Li, X. Bai, Y. Zhang, J. Phys. Chem. C 113 (2009) 16238–16246.

[52] A. Barkleit, S. Tsushima, O; Savchuk, J; Philipp, K; Heim, M; Acker, S; Taut, K. Fahmy, Inorg. Chem. 50 (2011) 5451–5459.

[53] X. L. Tan, X. K. Wang, H. Geckeis, TH. Rabung, Environ. Sci. Technol. 42 (2008) 6532–6537.

[54] X. L. Tan, Q. H. Fan, X. K. Wang, B. Grambow, Environ. Sci. Technol. 43 (2009) 3115–3121.

[55] F. Mercier, C. Alliot, N. Thromat, P. Toulhoat, Relat.Phenom. 150 (2006) 21–26.

[56] G. Sheng, H. Dong, R. Shen, Y. Li, Chem. Eng. J. 217 (2013) 486–494.

[57] F. Huang, Y. Zheng, Y. Yang, J. Appl. Polym. Sci. 103 (2007) 351–357.

[58] G. Montavon, C. Hennig, P. Janvier, B. Grambow, J. Colloid Interface Sci. 300 (2006) 482-490.

[59] A.G. Mirochnik, N.V. Petrochenkov, J. Lumin. 134 (2013) 906-909.

[60] V. A. Smirnov, G. A. Sukhadolski, O. E. Philippova, A. R. Khokhlov, J. Phys. Chem. B 103 (1999) 7621–7626.

Graphical abstract

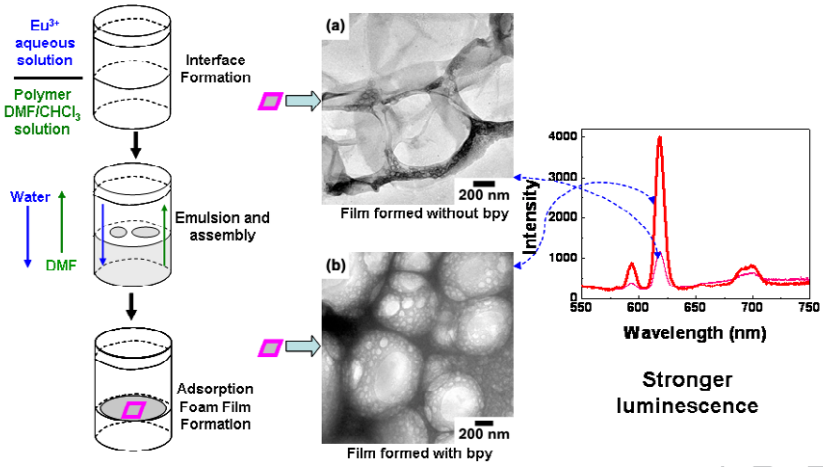

Highlights

► Composite films of block copolymer/Ln^{3+} were fabricated at liquid/liquid interfaces.
► Eu^{3+} and La^{3+} have great effects on morphologies and microstructures of the films.
► Polymer/Eu^{3+} and polymer/Eu^{3+}/bpy films exhibit good luminescent properties.